Electronic Supplementary Material (ESI) for Physical Chemistry Chemical Physics.

Electronic Supplementary Information

Excited-state relaxation of the solar cell dye D49 in organic solvents and on mesoporous Al_2O_3 and TiO_2 thin films

Oliver Flender, Mirko Scholz, Johannes R. Klein,

Kawon Oum and Thomas Lenzer**

Universität Siegen, Physikalische Chemie, Adolf-Reichwein-Str. 2, 57076 Siegen, Germany,
E-mail: oum@chemie.uni-siegen.de, lenzer@chemie.uni-siegen.de

Table of Contents

Concentration-dependent steady-state absorption spectra of D49

Figures S1 shows normalised steady-state absorption spectra of D49 in acetonitrile at three different concentrations. The $S_0 \rightarrow S_1$/ICT band with a peak at 472 nm (black line) exhibits a shift to shorter wavelengths with decreasing dye concentration. The effect is particularly pronounced at the lowest concentration of 3.3 x 10^{-6} M (peak at 417 nm, green line). It arises from deprotonation of D49. The acid-base equilibrium of the dye can be shifted to the acid side by adding a small amount of acetic acid. The result is shown in Fig. S2. In this case, we added 5 and 7 µL acetic acid to 3 mL of solutions with the concentrations 3.3 x 10^{-5} M and 3.3 x 10^{-6} M, respectively. The 3.3 x 10^{-4} M solution was left unchanged. All three curves coincide perfectly. This indicates that we observe the spectrum of the pure acid form of D49. In addition, this proves that there are no aggregation effects in this concentration range. Formation of J or H aggregates would shift the spectra to longer or shorter wavelengths, respectively, likely accompanied by the appearance of a broad and asymmetric band shape. This is obviously not the case. We note that the PSCP experiments were always carried out in the "high concentration" regime, so there was no need for the addition of acetic acid. This was confirmed by steady-state absorption spectra of the solutions recorded prior to the transient absorption measurements. On the other hand, care must be exercised when recording steady-state fluorescence spectra of D49 solutions at low concentration. Thus in the fluorescence experiments we added small amounts of acetic acid in all cases to be sure that the equilibrium was on the acid side.

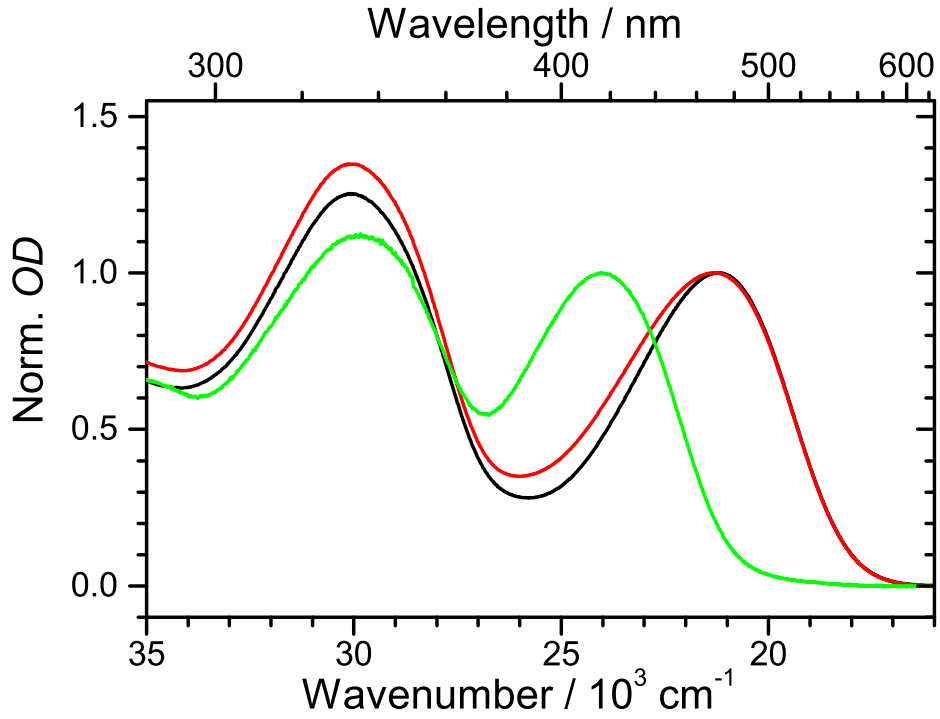

Fig. S1 Concentration-dependent steady-state absorption spectra of D49 in acetonitrile. (black) 3.3 x 10^{-4} M, (red) 3.3 x 10^{-5} M, (green) 3.3 x 10^{-6} M. Spectra are normalised at the peak of the $S_0 \rightarrow S_1$/ICT transition.

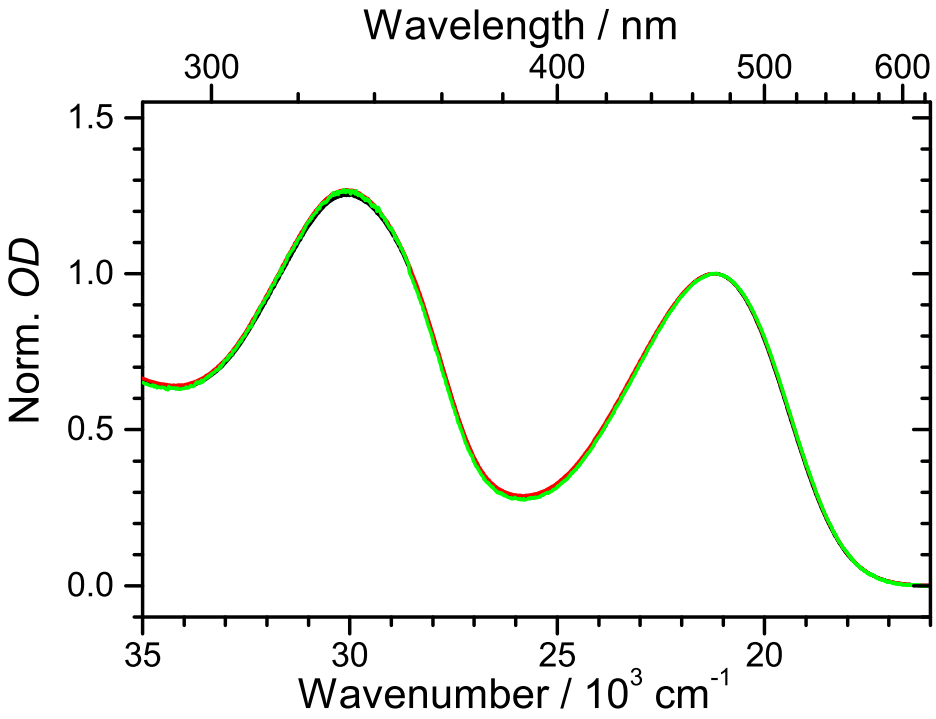

Fig. S2 Concentration-dependent steady-state absorption spectra of the D49 acid form in acetonitrile. (black) 3.3 x 10^{-4} M (3 mL), (red) 3.3 x 10^{-5} M (3 mL) + 5 µL acetic acid, (green) 3.3 x 10^{-6} M (3 mL) + 7 µL acetic acid. Spectra are normalised at the peak of the $S_0 \rightarrow S_1$/ICT transition and are corrected for the dilution effect assuming ideal mixing behaviour.

Cyclic voltammetry of D49

Figure S3 shows a cyclic voltammogram for the oxidation of D49 bound to a 500 nm thick mesoporous TiO_2 layer on FTO glass (red line). The cyclic voltammogram for the reference compound ferrocene is shown as a blue line. Oxidation of D49 produces the radical cation $D49^{\bullet+}$ and occurs at a voltage of 0.51 V *vs.* ferrocene^{+}/ferrocene (1.14 V *vs.* NHE). This is in excellent agreement with the value of Sun, Boschloo and co-workers.[1]

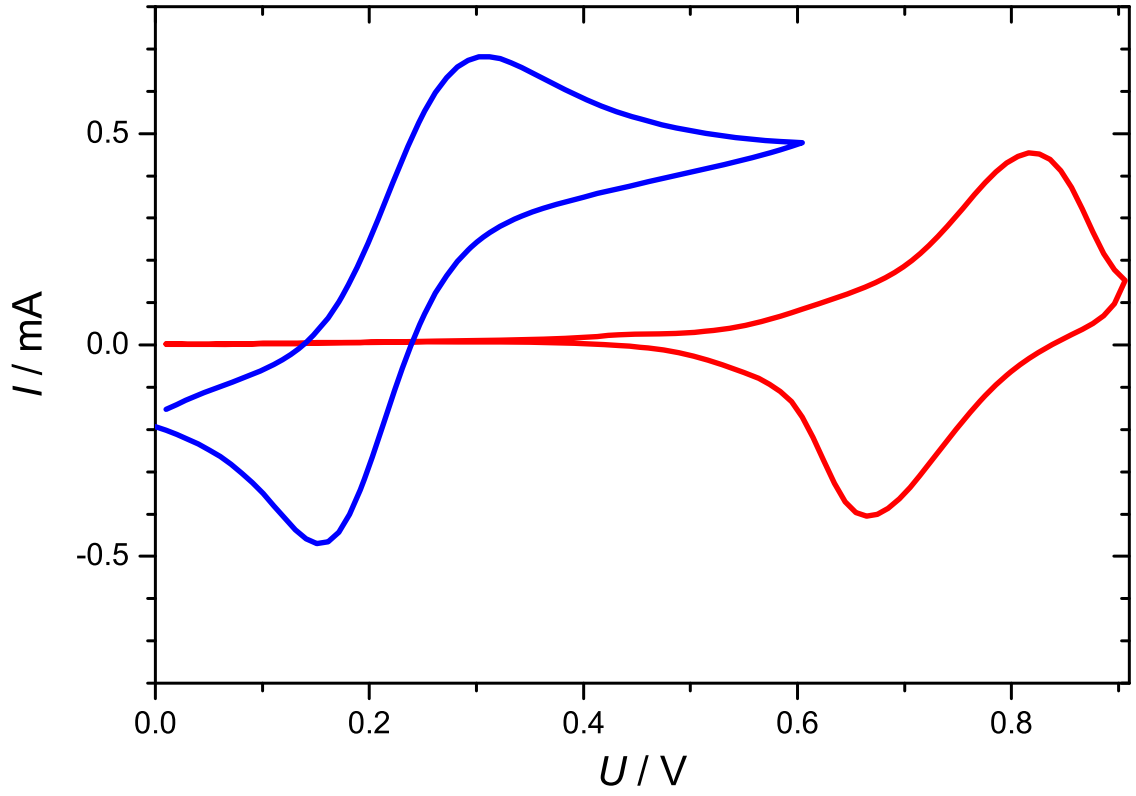

Fig. S3 Cyclic voltammograms for D49/TiO_2/FTO (red line) and ferrocene (blue line) at a scan rate of 0.1 V·s^{-1}.

UV-Vis-NIR broadband transient absorption spectra of D49

Figures S4-S9 summarise PSCP transient absorption spectra of D49 in three different organic solvents and on Al_2O_3, Al_2O_3/DCA and TiO_2. The corresponding contour plots for these transient spectra are included in Fig. 5 (main manuscript).

i) Diisopropyl ether

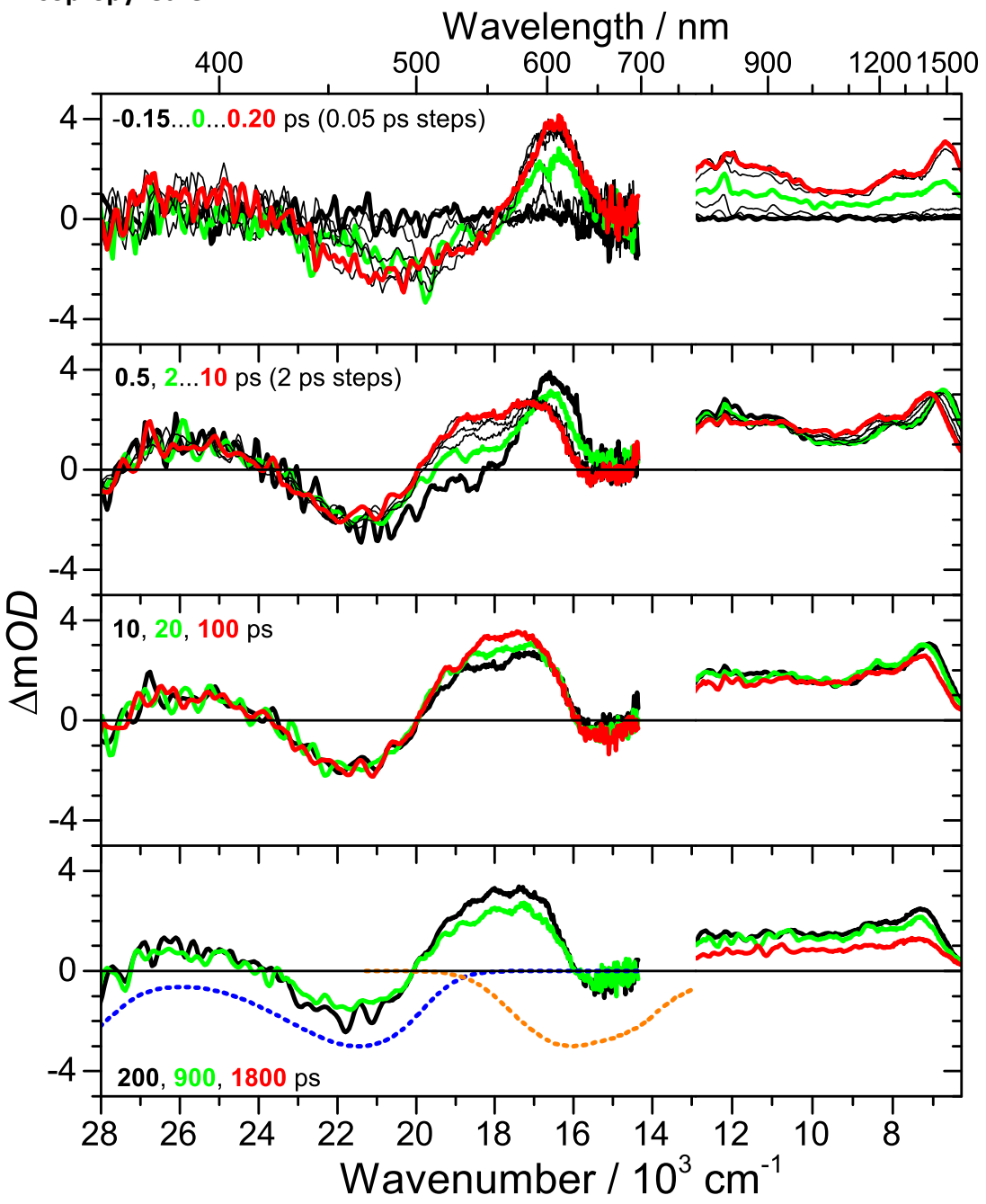

Fig. S4 PSCP transient absorption spectra of D49 in diisopropyl ether after photoexcitation at λ_{pump} = 505 nm. In the bottom panel, the inverted steady-state absorption spectrum (blue dashed line) and the steady-state stimulated emission spectrum (orange dashed line) are shown for comparison.

ii) THF

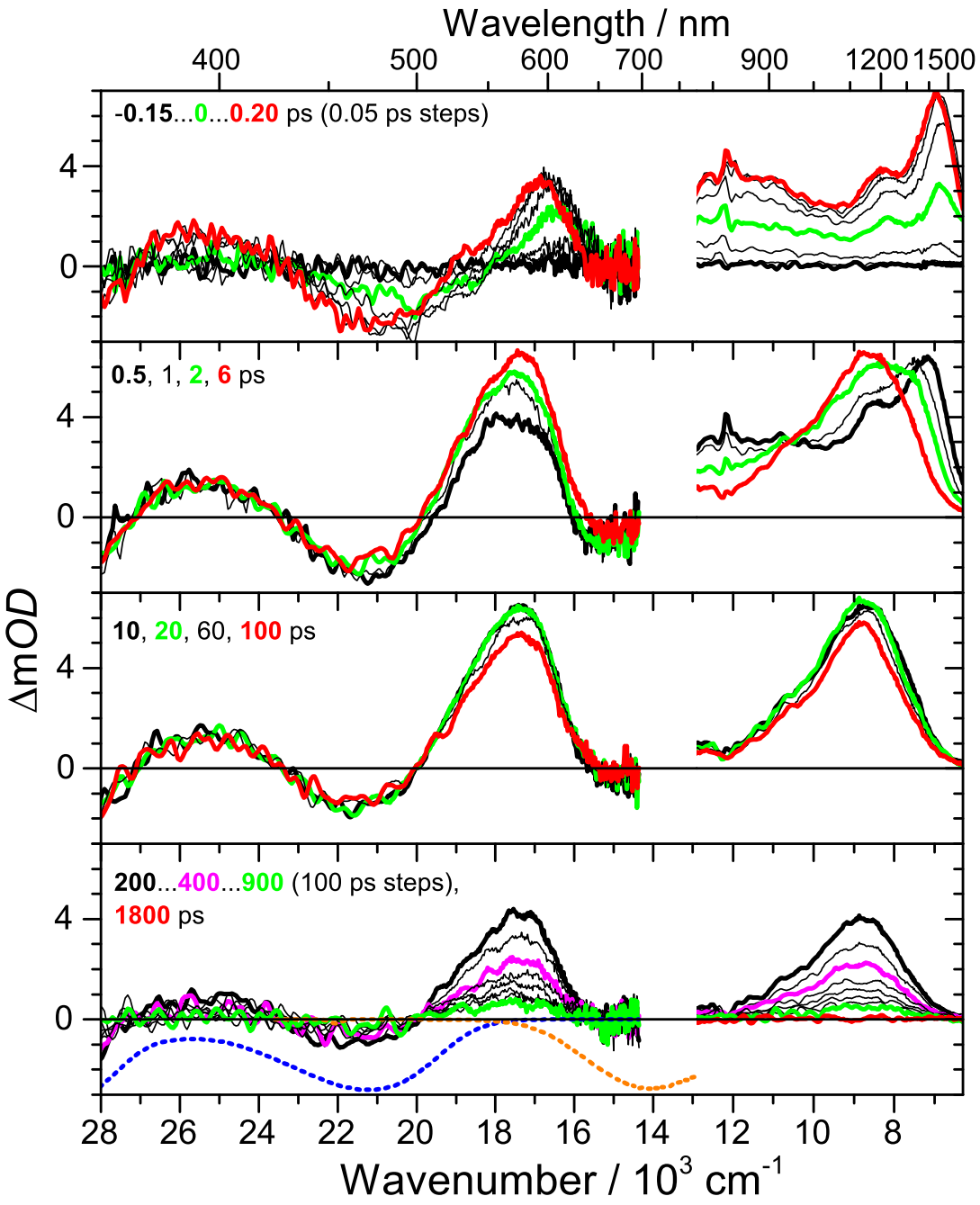

Fig. S5 PSCP transient absorption spectra of D49 in THF after photoexcitation at λ_{pump} = 505 nm. In the bottom panel, the inverted steady-state absorption spectrum (blue dashed line) and the steady-state stimulated emission spectrum (orange dashed line) are shown for comparison.

iii) Acetonitrile

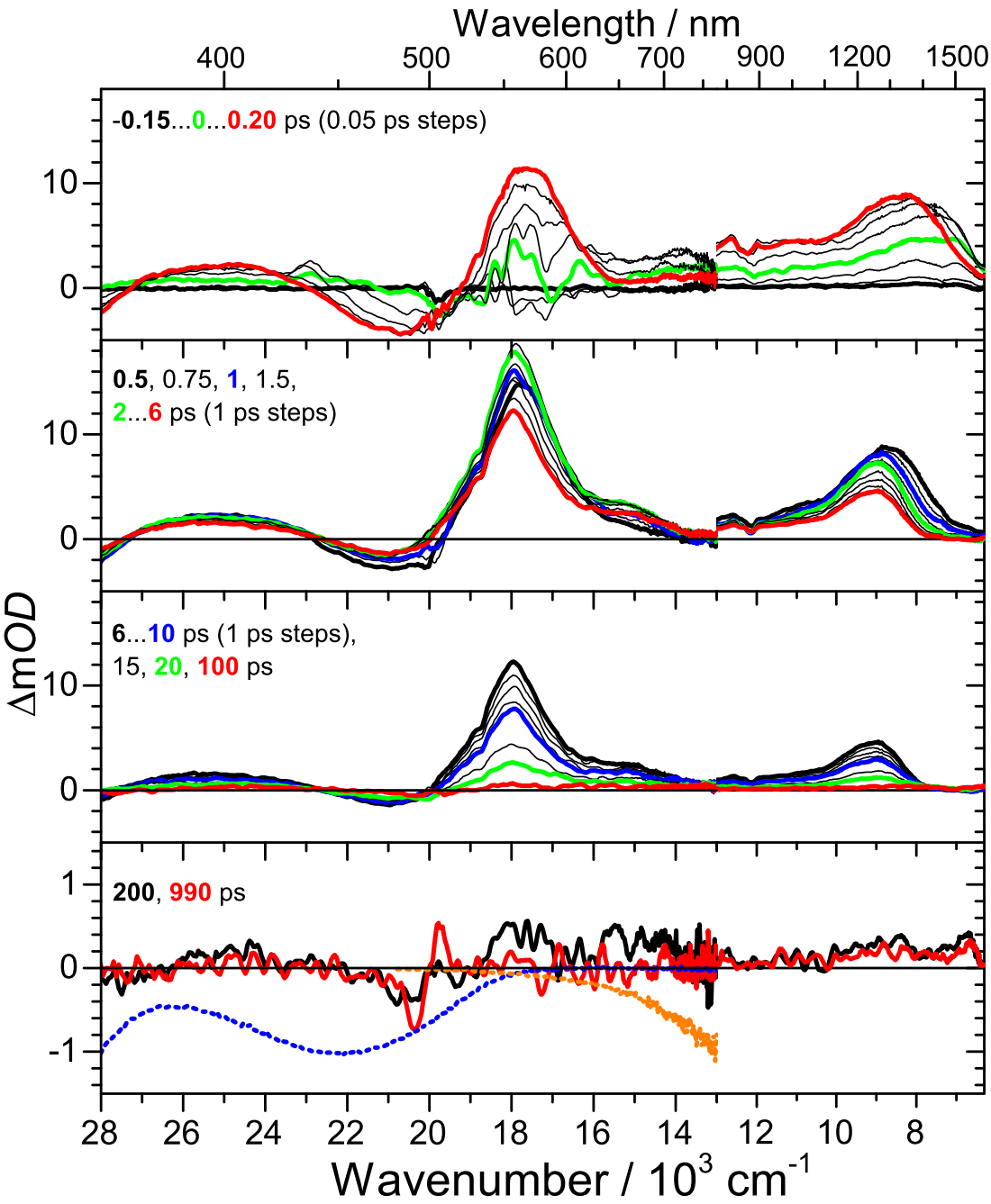

Fig. S6 PSCP transient absorption spectra of D49 in acetonitrile after photoexcitation at λ_{pump} = 505 nm. In the bottom panel, the inverted steady-state absorption spectrum (blue dashed line) and the steady-state stimulated emission spectrum (orange dashed line) are shown for comparison.

iv) Al_2O_3

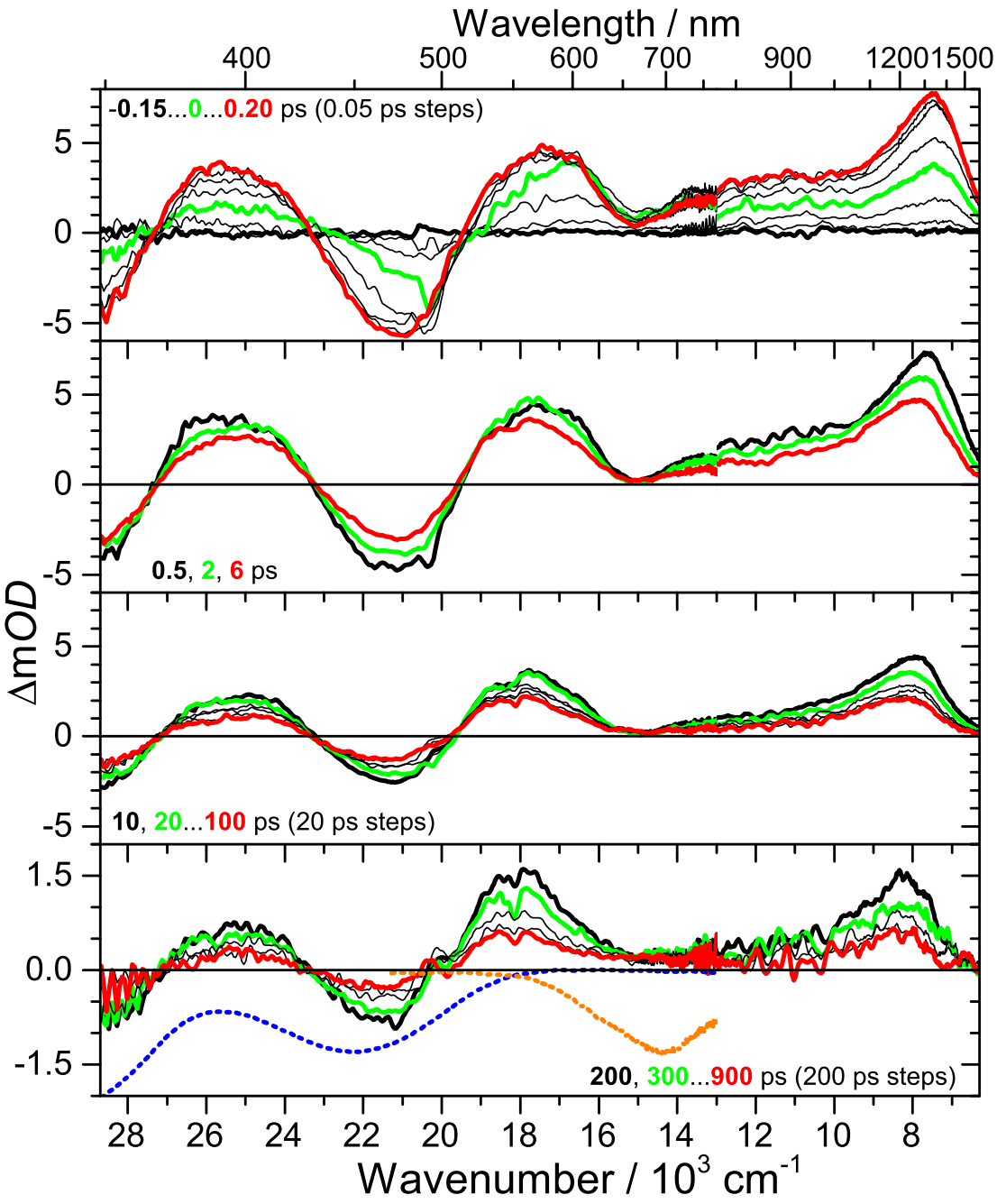

Fig. S7 PSCP transient absorption spectra of D49 on Al_2O_3 after photoexcitation at λ_{pump} = 505 nm. In the bottom panel, the inverted steady-state absorption spectrum (blue dashed line) and the steady-state stimulated emission spectrum (orange dashed line) are shown for comparison.

v) **Al_2O_3/DCA**

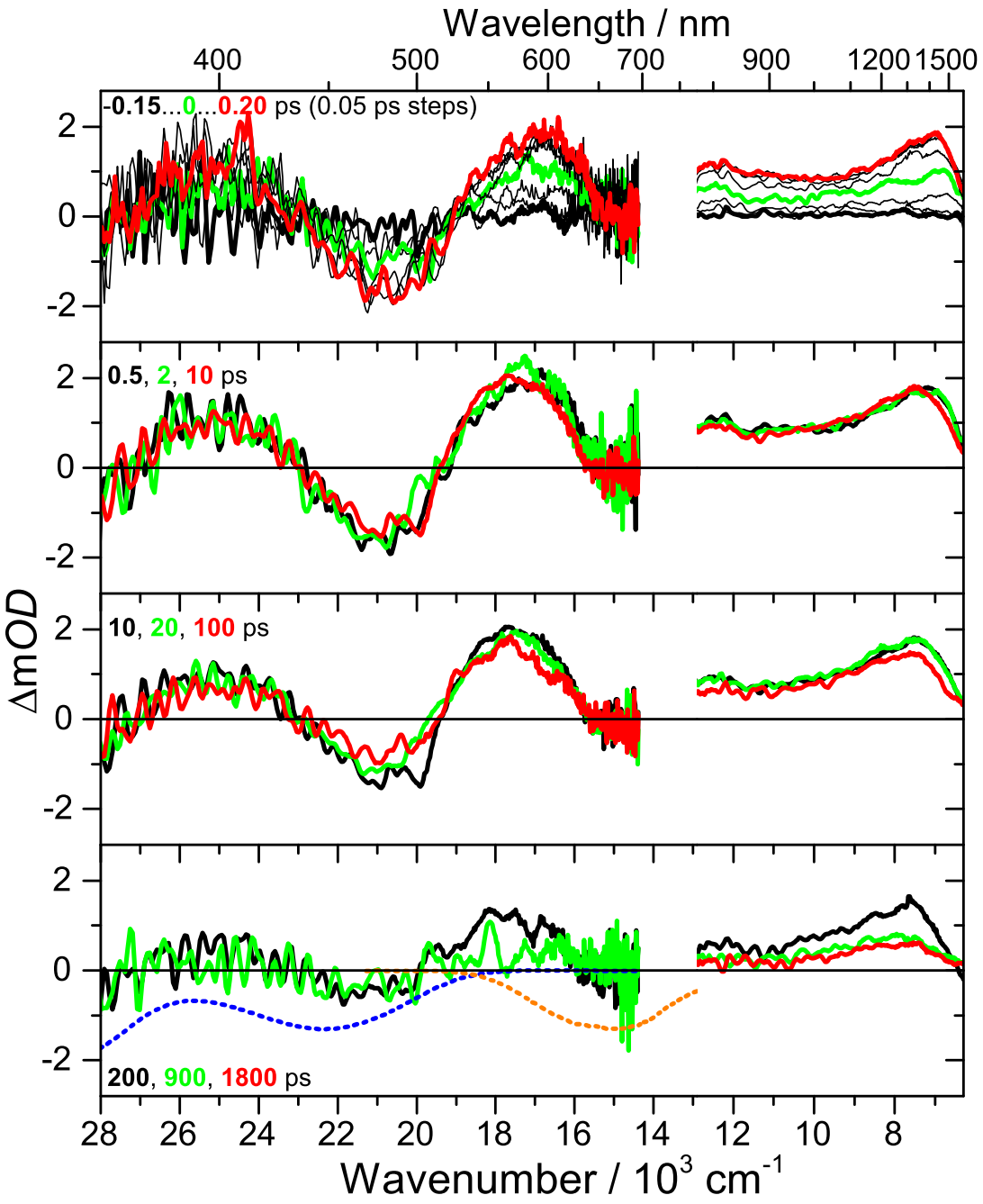

Fig. S8 PSCP transient absorption spectra of D49 on Al_2O_3/DCA after photoexcitation at λ_{pump} = 505 nm. In the bottom panel, the inverted steady-state absorption spectrum (blue dashed line) and the steady-state stimulated emission spectrum (orange dashed line) are shown for comparison.

vi) **TiO_2**

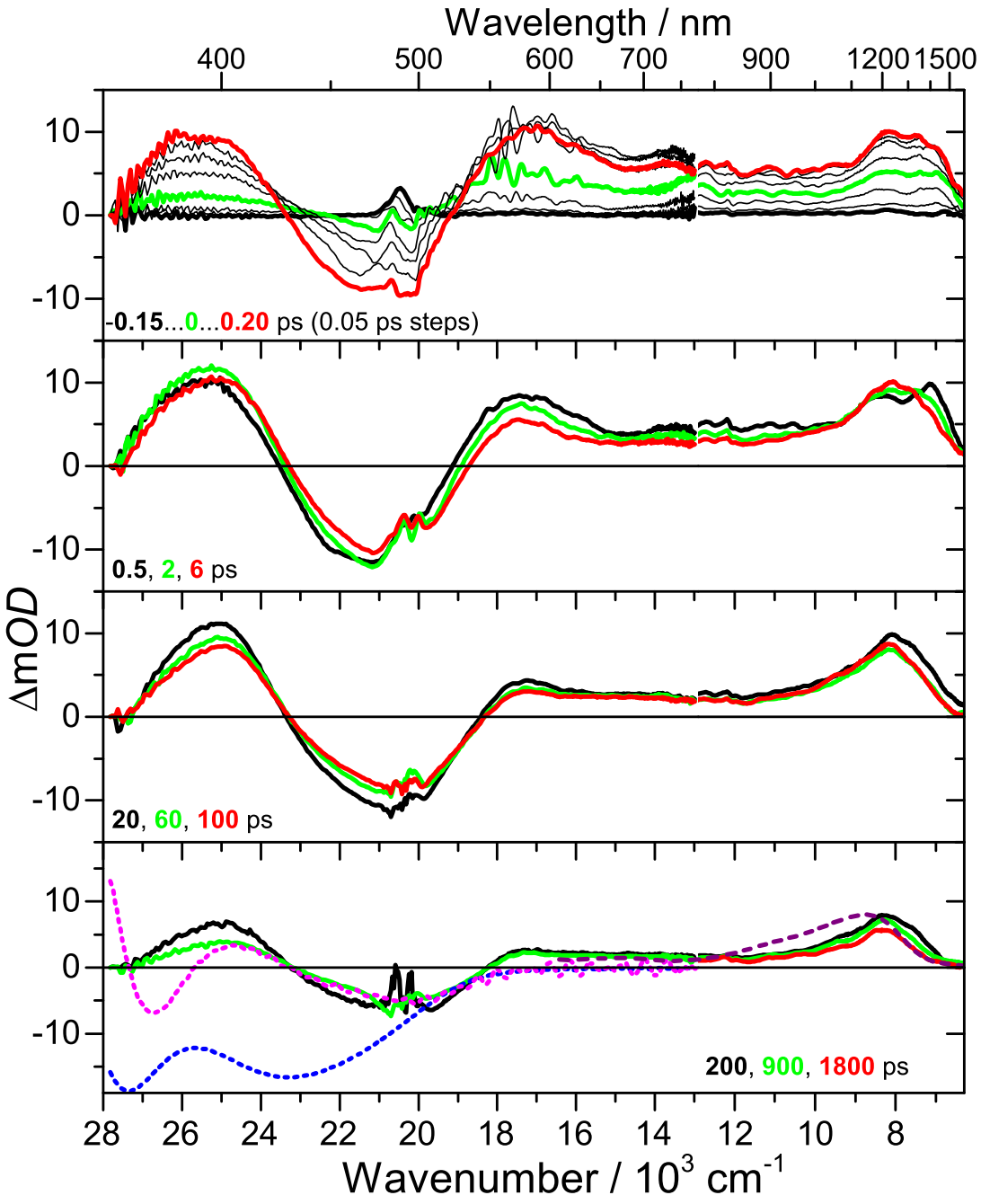

Fig. S9 PSCP transient absorption spectra of D49 on TiO_2 after photoexcitation at λ_{pump} = 505 nm. In the bottom panel, we also show the inverted steady-state absorption spectrum (blue dashed line), its scaled first derivative (magenta dashed line) and the steady-state Vis-NIR spectrum of the radical cation $D49^{\bullet+}$ on TiO_2/FTO from spectroelectrochemistry (purple dashed line; see also Fig. 4, main manuscript). Noise around 500 nm is due to residual straylight of the pump laser beam which cannot be perfectly subtracted.

Comparison of D49-sensitised Al_2O_3 thin films with and without prior DCA saturation

Figure S10 shows steady-state absorption (solid lines) and fluorescence spectra (dotted lines) of D49 on mesoporous Al_2O_3 thin films. Details of the film preparation were already presented in Sec. 2.1 (main manuscript). The spectra shown as red lines were obtained after saturating the film with D49 solution for three days. For recording the black spectra, the film was first saturated with DCA solution for two days and afterwards dipped into a D49 solution for three days ("two-step method").

The red shift of the absorption and fluorescence spectra and the considerably smaller fluorescence intensity of the pure D49 film are due to the larger surface polarity of D49 compared with DCA. Nonradiative relaxation accelerates and reduces the fluorescence quantum yield (assuming similar radiative lifetimes of D49 in the different environments). This behaviour is consistent with the much shorter lifetime of D49 in polar solvents determined in the broadband transient absorption experiments.

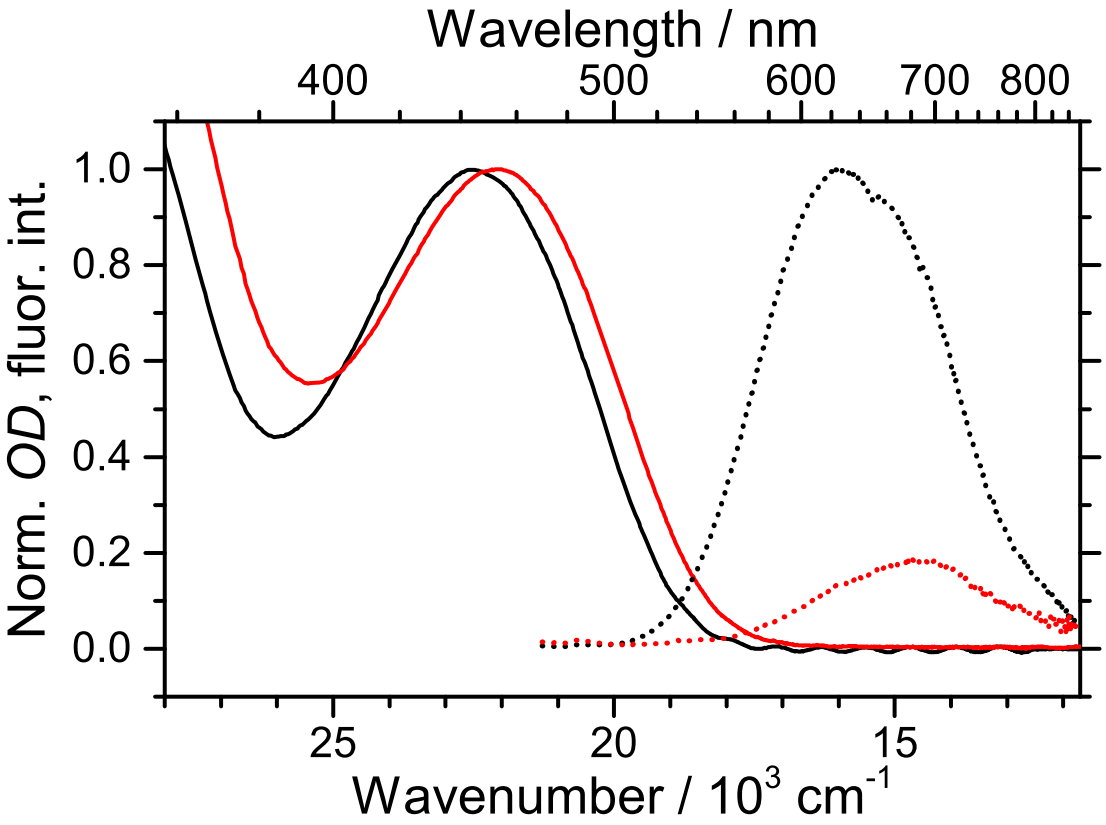

Fig. S10 Steady-state absorption spectra (solid lines) and fluorescence spectra (dotted lines) of D49 on Al_2O_3. (red) Al_2O_3 was saturated with a D49 solution for three days. (black) Al_2O_3 was saturated with a DCA solution for two days and subsequently placed in a D49 solution for three days. The two absorption spectra and the fluorescence spectrum (black dotted line) are normalised at the maximum. The fluorescence spectrum shown as a red dotted line is scaled to reproduce the experimentally observed reduction in emission intensity.

One-step co-adsorption of D49 and DCA on Al_2O_3 thin films

We also investigated films prepared *via* "one-step" co-adsorption methods. Solutions with a well-defined initial D49:DCA mole ratio were brought in contact with the Al_2O_3 thin film. Such procedures have been used in previous studies, *e.g.* to adsorb the indoline dye D131 together with DCA on Al_2O_3.[2]

First, we studied the D49 absorption spectra in solution for different D49:DCA mole ratios. The results in *i*-propanol (1:0, 1:15, 1:100, 1:400) are shown in Fig. S11 and corresponding spectra in *tert*-butyl alcohol / acetonitrile (1/1 by volume) for 1:0, 1:10 and 1:200 are presented in Fig. S12. In the case of *i*-propanol, the $S_0 \rightarrow S_1$/ICT band of D49 with a peak at *ca.* 440 nm gradually shifts with increasing DCA concentration. The spectrum at D49:DCA = 1:400 is significantly red-shifted. The behaviour is different for the *tert*-butyl alcohol / acetonitrile mixture. Here the pronounced red-shift is already reached at 1:10, with further addition of DCA up to 1:200 resulting in identical spectra.

In both cases the higher-energy electronic bands in the UV region do not shift and have very similar shapes. This suggests that the dye molecules do not aggregate upon addition of DCA. Therefore the absorption red-shift of the $S_0 \rightarrow S_1$/ICT band must arise from solvation, namely a decrease in the local polarity around the dye due to the increase in DCA concentration, compare *e.g.* D49/*n*-hexane in Fig. 2 (main manuscript). Obviously, a smaller amount of DCA is sufficient in the *tert*-butyl alcohol / acetonitrile mixture to cause the same amount of red-shift. This suggests a stronger interaction of DCA with D49, resulting in a local enrichment already at lower DCA concentration.

Figure S13 shows steady-state spectra for Al_2O_3 thin films with different D49:DCA mole ratios produced *via* the "one-step" route in *i*-propanol. Fluorescence of low-*OD* films is higher, whereas it is reduced for high-*OD* films. This is consistent with our findings for films prepared by the "two-step" route. However, we observed inferior batch-to-batch reproducibility for the spectra of "one-step" samples. Therefore the method was abandoned.

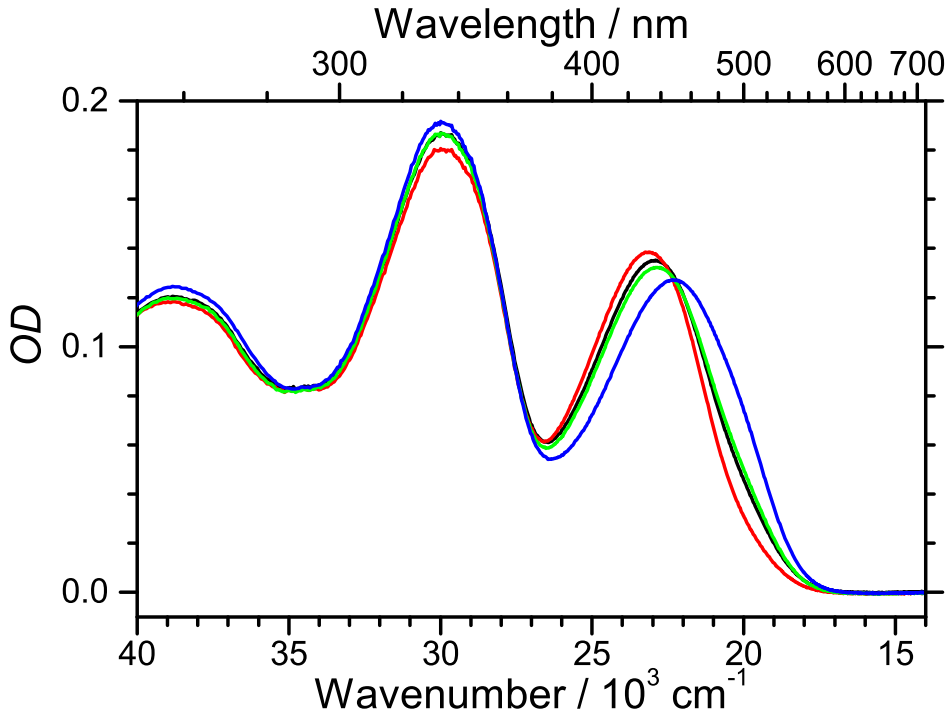

Fig. S11 Steady-state absorption spectra of *i*-propanol solutions with different D49:DCA mole ratios. (black) 1:0, (red) 1:15, (green) 1:100, (blue) 1:400.

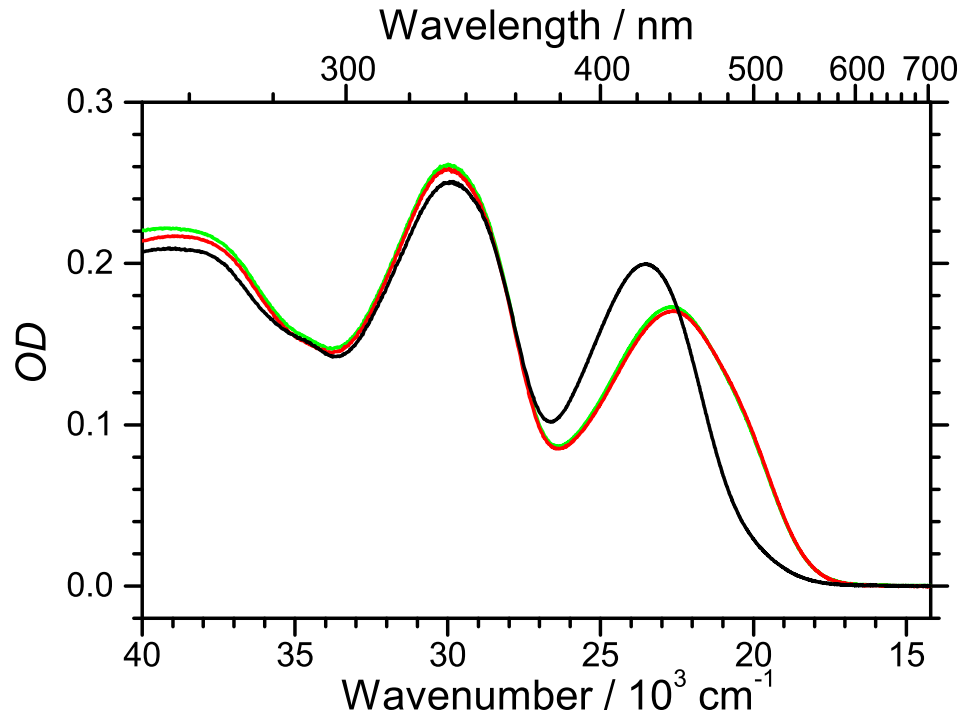

Fig. S12 Steady-state absorption spectra of *tert*-butyl alcohol / acetonitrile solutions with different D49:DCA mole ratios. (black) 1:0, (red) 1:10, (green) 1:200.

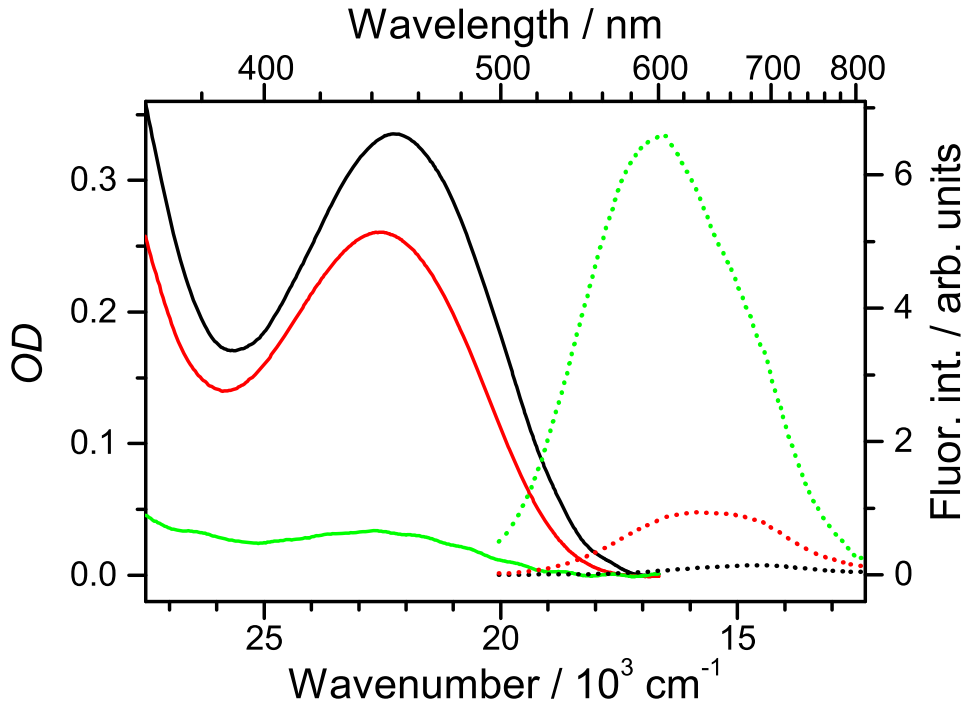

Fig. S13 Steady-state absorption spectra (solid lines) and fluorescence spectra (dotted lines) of D49/DCA-covered Al_2O_3 thin films prepared by the "one-step" method in *i*-propanol. D49:DCA mole ratios in the co-adsorbent solution: (black) 1:0, (red) 1:10, (green) 1:200.

Results of DFT/TDDFT calculations for D49, D49$^{\bullet-}$ and D49$^{\bullet+}$

Electronic transitions and oscillator strengths of neutral D49, the radical anion D49$^{\bullet-}$ and the radical cation D49$^{\bullet+}$ are summarised in Table S1. Corresponding gas-phase values for D49 and D49$^{\bullet+}$ can be found in our previous study on the dye E6.[3] Solvation by acetonitrile results in a red-shift relative to the gas-phase value and thus a stabilization of the first electronically excited state S_1/ICT relative to S_0. In contrast, for the radical anion and radical cation species a blue-shift is observed which suggests a larger stabilization of the D_0 state relative to the D_1 state.

Table S1 Wavenumber $\tilde{\nu}$ and oscillator strength f from DFT/TDDFT calculations for the ten energetically lowest excited state transitions of the radical anion D49$^{\bullet-}$ ($D_0 \rightarrow D_n$, gas phase and acetonitrile), the radical cation D49$^{\bullet+}$ ($D_0 \rightarrow D_n$, acetonitrile) and the five lowest states of neutral D49 ($S_0 \rightarrow S_n$, acetonitrile) using the MPW1K functional.

	D49$^{\bullet-}$ (Gas phase)		D49$^{\bullet-}$ (Acetonitrile)		D49$^{\bullet+}$ (Acetonitrile)		D49 (Acetonitrile)	
State	$\tilde{\nu}$ / cm^{-1}	f	$\tilde{\nu}$ / cm^{-1}	f	$\tilde{\nu}$ / cm^{-1}	f	$\tilde{\nu}$ / cm^{-1}	f
1	15500	0.17	17516	0.05	10940	0.60	20641	1.23
2	15961	0.02	19611	0.00	11629	0.24	28552	0.27
3	18504	0.00	21106	0.51	14457	0.30	31370	0.24
4	19552	0.02	21797	0.70	18361	0.10	32032	0.69
5	19604	0.68	24662	0.01	19957	0.01	32988	0.17
6	20790	0.16	25463	0.04	20665	0.00	---	---
7	21688	0.03	25602	0.00	22175	0.25	---	---
8	22033	0.07	26023	0.02	22500	0.22	---	---
9	22096	0.03	27152	0.11	23012	0.00	---	---
10	22858	0.02	27267	0.01	23258	0.10	---	---

References

1. Y. Hao, E. Gabrielsson, P. W. Lohse, W. Yang, E. M. J. Johansson, A. Hagfeldt, L. Sun and G. Boschloo, *Adv. Sci.*, 2015, **2**, 1500174.
2. U. B. Cappel, D. Moia, A. Bruno, V. Vaissier, S. A. Haque and P. R. F. Barnes, *Sci. Rep.*, 2016, **6**, 21276.
3. K. Oum, O. Flender, P. W. Lohse, M. Scholz, A. Hagfeldt, G. Boschloo and T. Lenzer, *Phys. Chem. Chem. Phys.*, 2014, **16**, 8019.